Direct Observation of the Transition State

JOHN C. POLANYI*

Department of Chemistry, University of Toronto, Toronto, Ontario, Canada M5S 1A1

AHMED H. ZEWAIL*

Arthur Amos Noyes Laboratory of Chemical Physics, California Institute of Technology,† Pasadena, California 91125

Received December 14, 1994

I. Introducing the Transition State

The direct observation of the "transition state" for chemical reaction clearly merits a place in this series devoted to the "Holy Grails" of chemistry. The transition state is neither one thing, namely, chemical reagents, nor the other, reaction products. Instead it illustrates the mystical event of trans-substantiation.

The time required for the electronic process of bond rupture and bond formation would be unmeasurably short were it not for the fact that the electronic transformations are triggered by substantial changes in internuclear separation. This became evident in the early years of quantum mechanics when it was possible, for the first time, to calculate the binding energy between an atomic pair, BC, as a function of internuclear separation.[1]

This seminal quantum calculation was rapidly extended to the case of three interacting particles[2] such as one encounters for the simple exchange reaction,

$$A + BC \rightarrow AB + C \qquad (1)$$

However, the step from the physics of AB and BC to the chemistry of ABC necessitated approximations so severe that the empiricism of Henry Eyring and Michael Polanyi was needed in order to render the first "potential energy surface" (PES) for a chemical reaction credible.[3]

The first PES for a reactive process, as anticipated since the time of Arrhenius, showed the reagents approaching, crossing an energy barrier, and then descending the far side of that barrier as the products separated. The whole trip from reagents to products involved changes in internuclear separation totaling ~10 Å. If the atoms moved at 10^4–10^5 cm/s, then the entire 10 Å trip would take 10^{-12}–10^{-11} s. If the "transition state", $[ABC]^{\ddagger}$, is defined to encompass *all configurations of ABC significantly perturbed from the potential energy of the reagents A + BC or the products AB + C*, then this period of 1–10 ps is the time available for its observation.

In fact, of course, the interest for the reaction dynamicist lies in the manner in which $[ABC]^{\ddagger}$ evolves from a species resembling reagent to one resembling product. Consequently the intervals at which one needs to record its configuration and energy are ~1% as great as that indicated above: in the range 10^{-14}–10^{-13} s (10–100 fs). Observation of a labile intermediate in this time interval is, therefore, the task of the transition state spectroscopist.

In the time domain, if the resolution is sufficiently short and the zero of time sufficiently well established, it is possible to clock the transition state in real time and to follow the nuclear motion. The key here is the ability to localize the reactive system to a spatial resolution of about 0.1 Å or less. Such localization refers quantally to a wave packet, a concept introduced in the early days of quantum mechanics by Schrödinger and Heisenberg.

The definition of the transition state (TS) used here, namely the full family of configurations through which the reacting particles evolve *en route* from reagents to products, may seem broad to those accustomed to seeing the TS symbol, ‡, displayed in solitary splendor at the crest of the energy barrier to reaction. It should be recognized, however, that even if one restricts one's interest to the overall rates of chemical reactions, one requires a knowledge of the family of intermediates sampled by reagent collisions of different collision energy, angle, and impact parameter. The variational theory of reaction rates further extends the range of TS of interest, quantum considerations extend the range yet further, and the concern with rates to yield products in specified quantum states and angles extends the requirements most of all. A definition of the TS that embraces the entire process of bond breaking and bond making, as used here, is therefore likely to prove the most enduring.

II. Characterizing the Transition State

Not surprisingly, transition state spectroscopy (TSS) began in the inverse domain of frequency, before moving on to the time domain. It was also to be expected, given the gradually evolving nature of science, that TSS would have its roots in a well-established field. At a time when the feasibility of TSS was the subject of vigorous debate, it was remarked that "the best sign that something is in reach in science is that, from a selected vantage point it can already be regarded as having been achieved".[4] Reference was being made to the fact that early in the century Lorentz had established that the broadening of the line spectrum of an atom A was due to the

John Polanyi received his training at Manchester University. Subsequently he was a postdoctoral fellow at the National Research Council in Ottawa (1952–1954) and at Princeton University (1954–1956). He has been at the University of Toronto since that date, with scientific interests in reaction dynamics, transition state spectroscopy, and surface-aligned photochemistry. In 1986 he shared the Nobel prize in chemistry with D. R. Herschbach and Y. T. Lee.

Ahmed Zewail received his B.S. from the University of Alexandria and his Ph.D. from the University of Pennsylvania. After two years of postdoctoral (IBM) fellowship at the University of California at Berkeley, he joined the faculty at Caltech, where he holds the Linus Pauling Chair in Chemistry and Physics. His current scientific interests are in the development of ultrafast laser techniques and their applications in chemistry and biology.

† Contribution No. 9023 from Caltech.

(1) Heitler, H.; London, F. *Z. Phys.* **1927**, *44*, 455.
(2) London, F. *Probl. Mod. Phys.* (Sommerfeld Festschrift) **1928**, 104; *Z. Elektrochem.* **1929**, *35*, 552.
(3) Eyring, H.; Polanyi, M. *Z. Phys. Chem.* **1931**, *B12*, 279.
(4) Polanyi, J. C. *Faraday Discuss. Chem. Soc.* **1979**, *67*, 129.

0001-4842/95/0128-0119$09.00/0

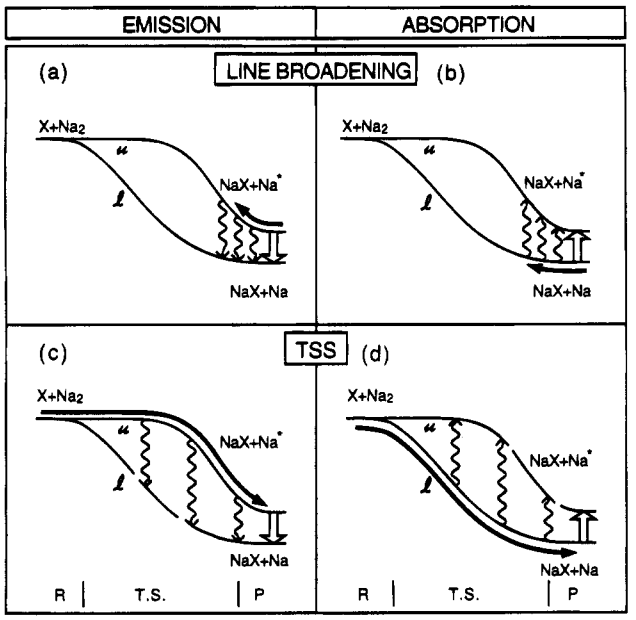

Figure 1. Panels a and b show the origins of collisional line broadening in emission and absorption (respectively) for collisions between sodium atoms and sodium halides; panels c and d show the comparable phenomenon of "transition state spectroscopy" (TSS) in emission and absorption for the case in which sodium atoms and sodium halides are formed in the chemical exchange reaction $X + Na_2 \rightarrow NaX + Na^*$ (reaction on the upper potential, u) or alternatively $X + Na_2 \rightarrow NaX + Na$ (reaction on the lower potential, l). The symbols R, TS, and P indicate the reagent, transition state, and product regions along the reaction coordinate. This figure is based on Figure 12 of ref 4.

fleeting interaction of A with a collision partner B, yielding a sufficient concentration of what today we might call transition states $[AB]^\ddagger$ in order to interact with light, i.e., give rise to TSS.

Each frequency in the Lorentzian "wing" of the atomic line corresponds to an internuclear separation r_{AB}. Frequencies further removed from the line center correlate in general with smaller r_{AB}. The longer $(AB)^\ddagger$ remains at a given r_{AB}, the more intense the emission or absorption at the corresponding frequency. Here, in 1915, was TSS in the frequency domain.[5] The broad wings, corresponding to a wide range of collisional internuclear separations r_{AB}, observed with modern instrumentation give clear evidence of the possibilities for TSS.[6]

All that would be needed in order to transpose this into the TSS sought by the reaction dynamicist would be that the collision be altered to one involving reactive collision partners, A + BC, or reaction products, AB + C. The upper panels of Figure 1 illustrate this for the case of sodium halide plus atomic sodium (AB + C) reaction products; the intensity of emission, $u \rightarrow l$, or absorption, $l \rightarrow u$, in the wing of the sodium atom resonance line gives a measure of the time that the TS spends in the configuration where the upper and lower potentials are separated by ν.[4]

Transition state spectroscopy began in what laser spectroscopists would characterize as a continuous wave (CW) mode, in which a distribution of spectral frequencies provided the clue to the desired information regarding the distribution of the TS over successive configurations and potential energies. We shall refer first to this approach and later (section III) to the clocking of the evolution of the TS directly in the time domain.

Not surprisingly, the young field of TSS involves a number of studies of alkali metal atoms. Previously alkali metals had provided a proving ground for collisional line broadening[6] as well as for the study of simple exchange reactions.[7] Accordingly, the first TSS experiments involved alkali metal atomic exchange reactions, studied at pressures that were orders of magnitude lower than those at which collisional pressure broadening would normally be observed. Nonetheless there was undoubted evidence of far-wing emission[8] and absorption[9] extending ~100 nm away from the alkali metal atom line center. This was indicative of the occurrence of a strong collision.[6,10] The "collision" in question was that between the products of reactions 2 and 3 (see refs 8 and 9),

$$F + Na_2 \rightarrow NaF + Na^* \qquad (2)$$

and

$$K + NaCl + h\nu \rightarrow KCl + Na^* \qquad (3)$$

as illustrated schematically for reaction $X + Na_2$ in the lower panels of Figure 1.

In the case of reaction 2,[8] wings to the red and the blue of the D-line evidenced themselves in emission (see Figure 1c). The integrated intensity of the wing emission was $\sim 10^{-4}$ that of the sodium D-line emission (lifetime $\sim 10^{-8}$ s), giving a total lifetime for the $[FNa_2]^\ddagger$ of $\sim 10^{-12}$ s. For reaction 3,[9] laser absorption by $[KClNa]^\ddagger$, tens of nanometers to the red of the sodium D-line and also a little to the blue, was detected by recording the resulting D-line wavelength. The laser absorption is shown in the more detailed rendering of Figure 2, based on the *ab initio* calculations of Yamashita and Morokuma for this system.[11]

A limitation in both of these early experiments, as in line broadening in general, was the sparsity of structure in the wings. Early calculations[10] had shown that structure should be present, corresponding to the marked variation in density of TS species along the reaction coordinate. In recent work[12] on the exchange reaction K + NaBr, Brooks's laboratory has found clear evidence of structure centered 20 nm to the red of the sodium D-line, when one component of the line, D_2 ($^2P_{3/2} \rightarrow {}^2S_{1/2}$), is monitored but not when D_1 is the product. This structure in the TS spectrum was attributed to absorption of radiation by $[KBrNa]^\ddagger$ reacting by way of an electronically excited transition state. What happens, it appears, is that *en route* to forming $Na(D_2)$ the system hops to an excited PES and lingers there.

Without the aid of TSS this intermediate bifurcation of the reaction pathway might have escaped notice, making no more than a feeble imprint on the product attributes. Two different PES pathways to identical reaction products have in fact been identified previ-

(5) Lorentz, H. A. *Proc. K. Ned. Akad. Wet.* **1915**, *18*, 154.
(6) For a review, see: Gallagher, A. In *Spectral Line Shapes*; Burnett, K., Ed.; De Gruyter: Berlin, 1982; Vol. 2, p 755.
(7) Polanyi, M. *Atomic Reactions*; Williams and Norgate: London, 1932.
(8) Arrowsmith, P.; Bartoszek, F. E.; Bly, S. H. P.; Carrington, T., Jr.; Charters, P. E.; Polanyi, J. C. *J. Chem. Phys.* **1980**, *73*, 5895. Arrowsmith, P.; Bly, S. H. P.; Charters, P. E.; Polanyi, J. C. *J. Chem. Phys.* **1983**, *79*, 283.
(9) Hering, P.; Brooks, P. R.; Curl, R. F.; Judson, R. S.; Lowe, R. S. *Phys. Rev. Lett.* **1980**, *44*, 698. Brooks, P. R.; Curl, R. F.; Maguire, T. C. *Ber. Bunsen-Ges. Phys. Chem.* **1982**, *86*, 401. Brooks, P. R. *Chem. Rev.* **1988**, *88*, 407.
(10) Polanyi, J. C.; Wolf, R. J. *J. Chem. Phys.* **1981**, *75*, 5951.
(11) Yamashita, K.; Morokuma, K. *J. Phys. Chem.* **1988**, *92*, 3109; *J. Chem. Phys.* **1989**, *91*, 7477.
(12) Barnes, M. D.; Brooks, P. R.; Curl, R. F.; Harland, P. W.; Johnson, B. R. *J. Chem. Phys.* **1992**, *96*, 3559.

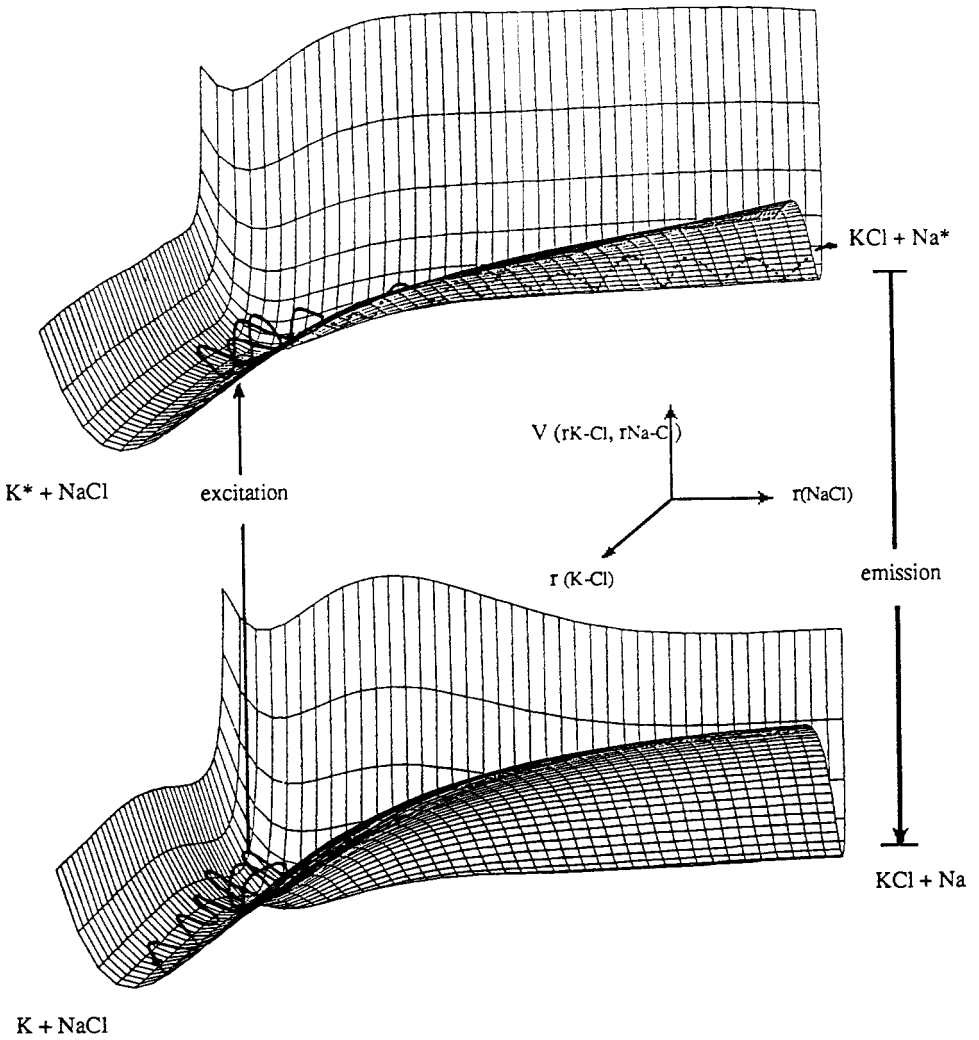

Figure 2. Potential energy surfaces for the ground state and excited state K + NaCl reactions, computed by Yamashita and Morokuma (ref 11). A schematic reactive trajectory originates in K + NaCl, approaches to the TS, and is photoexcited to $[K^*NaCl]^‡$; thereafter, this excited TS gives rise to KCl + Na* with subsequent D-line emission. Reprinted with permission from ref 12. Copyright 1992 American Institute of Physics.

ously by the observation of the product motions, gaining for the TS's of such reactions the description "microscopic branching".[13] In TSS, however we have a means of establishing where along the reaction coordinate the bifurcation begins, and how long it continues.

In the following section we compare some expedients that have been used in order to access the TS and characterize it in greater detail. Since the transition state is a "free" (unbound) state, its absorption spectrum will be most meaningful in the case that an electronic transition takes place to a bound state. The vibrational and rotational quantum levels in the bound electronic state, to the extent that they are known, will act as "markers" that assist in the location of energies and configurations in the state of interest, the transition state.

A simple example of free-to-bound TSS is to be found in the far-sighted experiments of Weiner and coworkers, who studied collisions between Li atoms by the laser absorption spectroscopy of the collision pair $[LiLi]^‡$, which was thereupon excited from its free state to the bound ionic Li_2^+.[14]

Studies of $[AB]^‡ + h\nu \rightarrow AB$, i.e., free-to-bound TSS, were performed at an early date by Setser and co-workers[15] on reactions such as $Xe + Br \rightarrow [XeBr]^‡$, which on laser irradiation was excited to the bound state, XeBr*. Their TSS showed unmistakable Franck–Condon structure due to peaks in the overlap between the nuclear wave functions for the free and the bound states. This structure assisted in the mapping of the free state $[XeBr]^‡$, the TS.[15]

Comparable "free-to-bound" experiments were proposed as a means to the observation of the transition state in the classic exchange reaction $H + H_2 \rightarrow [H_3]^‡ \rightarrow H_2 + H$.[16] Excitation of the free $[H_3]^‡$ would be to bound H_3*, and quantum states of this excited electronic state would provide markers along the TS reaction pathway in the ground state. The experiment has yet to be successfully performed. Despite the lingering of $H_3^‡$ at certain intermediate configurations, the reaction, as normally studied, proceeds through too wide a range of $[H_3]^‡$ geometries to permit TSS (see, however, section IV).

It has been shown that particularly rich structure can be obtained if one starts $[AB]^‡$, $[ABC]^‡$, etc. on their path to products from well-defined TS configurations. Experiments performed by Imre, Kinsey, and co-

(13) Polanyi, J. C. *Science* **1987**, *236*, 680.
(14) Hellfeld, A. V.; Caddick, J.; Weiner, J. *Phys. Rev. Lett.* **1978**, *40*, 1369.
(15) Ku, J. K.; Setser, D. W.; Oba, D. *Chem. Phys. Lett.* **1984**, *109*, 429.
(16) Mayne, H. R.; Poirer, R. A.; Polanyi, J. C. *J. Chem. Phys.* **1984**, *80*, 4025. Mayne, H. R.; Polanyi, J. C.; Sathyamurthy, N.; Raynor, S. *J. Phys. Chem.* **1984**, *88*, 4064.

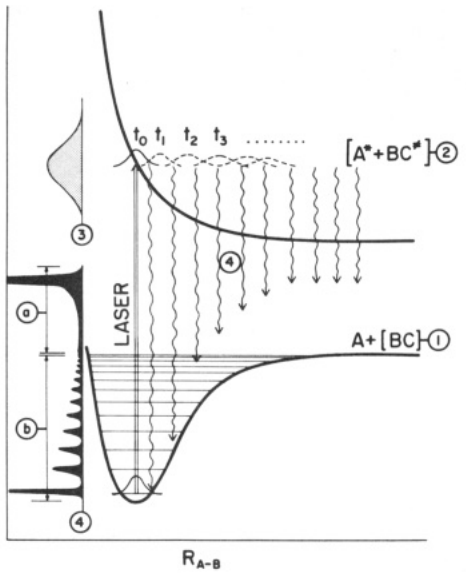

Figure 3. Bound-to-free laser excitation of stable ABC (curve 1) gives rise to dissociative $[ABC]^{\ddagger}$ on the repulsive upper potential curve (2). Curve 3 is the absorption spectrum. Curve 4 is the emission pictured as successive downward transitions and (at left) as the resultant spectrum ((a) unstructured, (b) structured). Reprinted with permission from ref 17b. Copyright 1984 American Chemical Society.

workers demonstrated this in an impressive fashion.[17] The free species (the TS) was formed in a narrow range of configurations by laser excitation of a bound molecule (Figure 3). During its stay in the free state the dissociating species emitted to quantum states of the ground electronic state, as determined by the Franck–Condon overlap for successive configurations as the TS dissociated to products.

This scenario for TSS was discussed concurrently for the simpler case of a dissociating diatomic, NaI*.[18] The Na* emission showed substantial far-wing emission. This was ascribed to emission by $[NaI]^{*\ddagger}$ *en route* to Na* + I. The story of NaI TSS will, however, be told in section III in terms of time-resolved spectroscopy, where it has been truly informative.

In recent years theoretical studies have shown both the power of this type of half-collision TSS to reveal the PES of the dissociating species and the problems inherent in making this connection. The power of the method has already been alluded to; the initial configuration is well-defined. The complexity arises from two sources: (i) for a polyatomic ($[CH_3I]^{\ddagger} \rightarrow CH_3 + I$ or $[O_3]^{\ddagger} \rightarrow O_2 + O$) the exit valley of the PES exists in a multicoordinate space; and (ii) since the dissociating TS is formed by photon absorption, it dissociates in an electronically excited state and may therefore explore intersecting electronic states *en route* to products. The first of these complications represents an opportunity, since in a favorable example characteristic series of spectral lines signal the nature and extent of excitation in the various coordinates linked to dissociation. The second complication could be significant since emission from differing electronically excited TS's might give rise to emission in similar spectral regions. Here time-resolved TSS will again be of value.

A further general method of forming TS's based on modern laser spectroscopy has been applied to a different sort of "half-reaction", namely, unimolecular dissociation in the ground electronic state. The starting material in the example to be cited was once again a stable uncharged molecule, HFCO.[19] The objective was to form internally excited HFCO with a known initial distribution over vib-rotational energy states. If the total internal energy exceeded the barrier height for unimolecular dissociation, this constituted a TS, $[HFCO]^{\ddagger}$. Its reaction was studied primarily by its rate of disappearance. A related approach has been used successfully to study the TSS for isomerization, a classic unimolecular process.[20] However, this narrative will stay with HFCO.

The $[HFCO]^{\ddagger}$ was formed by "pump" laser excitation to an energetic excited state followed by "dump" laser stimulated emission to a selected vib-rotational state of $[HFCO]^{\ddagger}$. There was evidence of extreme sensitivity of the unimolecular reaction rate to small changes in the energy distribution of the $[HFCO]^{\ddagger}$. An increase of only 0.012 kcal mol^{-1} in the TS rotational excitation resulted in an increase in the rate of dissociation by a factor of ~40 (from 16 to 650 ns). The form of motion in the TS appears to be crucial. It seems that through the Coriolis forces the increased rotation opens a gateway for out-of-plane bending to contribute substantial momentum to the (in-plane) dissociation of the TS.

In the examples being cited, the TS has been accessed (directly or indirectly) from a bound state that defines the internuclear separations. A powerful method for TSS that embodies this principle is to "complex" the reagents or their precursor prior to reaction. Since the complexed species are a few angstroms apart, following excitation by light the reaction proceeds from a TS to products.

In the first variant on this approach that we shall mention, the complex was a van der Waals cluster. The method being described was pioneered by Soep and co-workers using, for example, complexes Hg···Cl_2 or Ca···HCl.[21] Pulsed irradiation triggered reaction, by electronically exciting the metal atom. This approach has been extended to the classic alkali metal atom "harpooning" reactions, complexed as Na···XR (XR = organic halide).[22] A significant development is due to Wittig and co-workers,[23] who replaced the metal atom in the complex by a molecule that on photolysis aimed a photofragment along a preferred direction, with a somewhat restricted range of impact parameters, at the remainder of the complex. Thus the complex IH···OCO when irradiated with 193 nm UV released an H atom that reacted with the CO_2 end of the complex to yield OH whose internal energy was probed. This type of "spectroscopy starting in the TS" will be augmented by experiments in which the photolytic reagent and its reaction partner are held together more strongly at a defined separation, ori-

(17) (a) Imre, D.; Kinsey, J.; Field, R.; Katayama, D. *J. Phys. Chem.* **1982**, *86*, 2564. (b) Imre, D.; Kinsey, J. L.; Sinha, A.; Krenos, J. *J. Phys. Chem.* **1984**, *88*, 3956.

(18) Foth, H.-J.; Polanyi, J. C.; Telle, H. H. *J. Phys. Chem.* **1982**, *86*, 5027. Foth, H.-J.; Mayne, H. R.; Poirier, R. A.; Polanyi, J. C.; Telle, H. H. *Laser Chem.* **1983**, *2*, 229.

(19) Choi, Y. S.; Moore, C. B. *J. Chem. Phys.* **1992**, *97*, 1010.

(20) Chen, Y. T.; Watt, D. M.; Field, R. W.; Lehmann, K. K. *J. Chem. Phys.* **1990**, *93*, 2149. Field, R. W.; Ishikawa, H.; Rajaram, B.; Wang, J.; Chen, Y. T. *Proc. Welch Found. Conf. Chem. Res. XXXVIII*, Chemical Dynamics of Transient Species, Houston, TX, Oct 24–25, 1994.

(21) Jouvet, C.; Soep, B. *Chem. Phys. Lett.* **1983**, *96*, 426. Soep, B.; Whitham, C. J.; Keller, A.; Visticot, J. P. *Faraday Discuss. Chem. Soc.* **1991**, *91*, 191.

(22) Liu, K.; Polanyi, J. C.; Yang, S. *J. Chem. Phys.* **1992**, *96*, 8628; **1993**, *98*, 5431. Polanyi, J. C.; wang, J.-X.; Yang, S. H. *Isr. J. Chem.* **1994**, *34*, 55.

(23) Hoffman, G.; Oh, D.; Chen, Y.; Engel, Y. M.; Wittig, C. *Isr. J. Chem.* **1990**, *30*, 115.

entation, and angle by an underlying substrate, i.e., by studies of "surface aligned photochemistry" (see section IV).[24]

Among the most informative experiments using complexes to arrange the reagents in a TS configuration have been those in which the complex existed only as a negatively charged ion. This approach introduced by Neumark[25] is a form of emission spectroscopy. The emission, however, consists of not photons but electrons. The emission is triggered by light of fixed wavelength which transforms the stable complex ABC^- to the labile TS $[ABC]^‡$, resulting in the emission of electrons whose translational energies have imprinted on them the preferred energies of $[ABC]^‡$. These energies are vibrational modes approximately orthogonal to the reaction coordinate, and also resonances corresponding to quantum "bottlenecks" along the reaction pathway. The work began with the observation of vibrational modes in the TS's of hydrogen-transfer reactions, e.g., I + HI.[26]

The most telling case to have been studied in this way is the prototype of exothermic exchange reactions, $F + H_2 \rightarrow HF + H$.[27] The FH_2^- complex was formed by clustering F^- with both parahydrogen and normal hydrogen. The FH_2^- photoelectron spectra for the para complex and the ortho complex are shown in Figure 4. The spectra closely mirror the spectrum from an exact three-dimensional quantum reactive scattering calculation on a recent $F + H_2$ PES which, in contrast to earlier PES's, gives a markedly bent $[FHH]^‡$ TS configuration.

Most of the structure in Figure 4 can be attributed to bending motion in the TS; the linear FHH^- is projected into the TS region of the $F + H_2$ reaction where $[FHH]^‡$ prefers to be bent, thus exciting bending motion. The para and ortho cases are different since the former has only those bending states that correlate with reagent $F + H_2$ (J = even) and the latter those that correlate with $F + H_2$ (J = even and odd, in the ratio 3:1).

In addition to the clear evidence for vibration in the TS, there is a narrow peak in the para FH_2^- spectrum (theory and experiment, Figure 4) located at 1.044 eV, due to a scattering resonance, i.e., a quasi-bound state in the H + HF product valley. In this case the spectral feature is associated with motion more nearly along the reaction coordinate than perpendicular to it.

In closing this section we mention an intriguing analogue to photoelectron emission from the TS in which the TS *spontaneously* emits an electron. Morgner and co-workers[28] studied the system metastable $He^*(1s2s) + Br_2 \rightarrow [He^+ \cdots Br_2^-]^‡ \rightarrow He + Br + Br^+ + e^-$. This could be made more informative by complexing the inert gas and halogen prior to excitation so as to restrict the initial configurations.

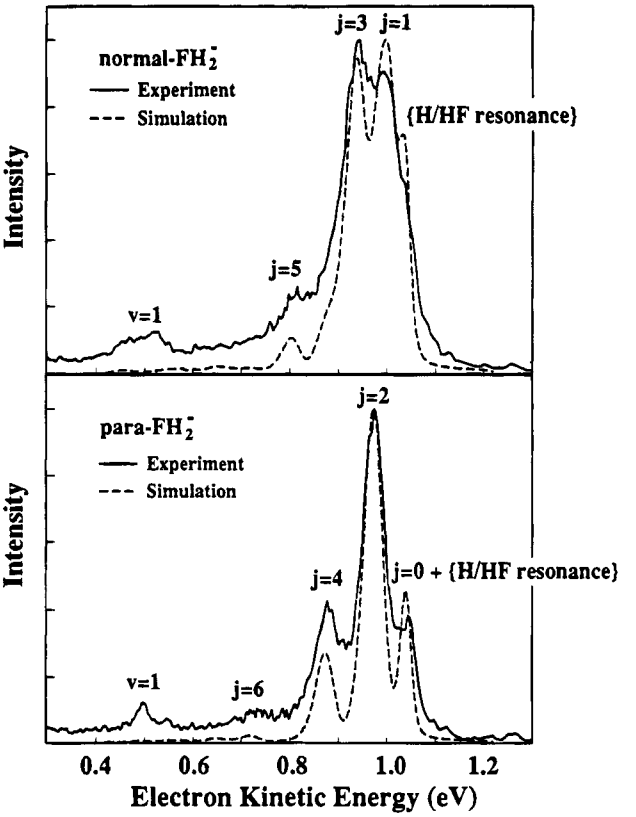

Figure 4. Comparison between the experimental (solid line) and the theoretical (broken line) photoelectron spectra of FH_2^-, for para FH_2, below, and normal FH_2^-, above. Reprinted with permission from ref 27. Copyright 1993 American Association for the Advancement of Science.

III. Clocking the Transition State

As noted in section I, the entire journey of a reaction, often involving a 10 Å configurational change, takes 1−10 ps. With ultrashort laser pulses, one is able to define the zero of time and follow the elementary dynamics of transition states, reaction rates, and energy redistribution.[29−36] On the femtosecond time scale the spatial resolution is narrowed to 0.1 Å or less and the reaction can be initiated with $t = 0$ defined to better than 10 fs.[29] This initial *coherent* localization allows for the visualization of the motion of the atoms as classical particles moving in time frames from reactants to products. Quantally, this corresponds to a wave packet motion. Such a concept of coherent, localized wave packets is fundamentally linked to the foundation of the uncertainty principle.

The femtosecond temporal resolution corresponds to uncertainty in the momentum, which in turn leads to the localization in space through $\Delta X \Delta P \sim \hbar$. Furthermore, one prepares the system coherently (and not one state at a time) and, in analogy with diffraction

(24) Polanyi, J. C.; Williams, R. J. *J. Chem. Phys.* **1988**, *88*, 3363. Polanyi, J. C.; Rieley, H. In *Dynamics of Gas-Surface Interactions*; Rettner, C. T., Ashfold, M. N. R., Eds.; Royal Society of Chemistry: London, Rettner, C. T., Ashfold, M. N. R., Eds.; 1991; Chapter 8, p 329.

(25) Metz, R. B.; Bradforth, S. E.; Neumark, D. M. *Adv. Chem. Phys.* **1992**, *81*, 1. Neumark, D. M. *Acc. Chem. Res.* **1993**, *26*, 33.

(26) Weaver, A.; Metz, R. B.; Bradforth, S. E.; Neumark, D. M. *J. Phys. Chem.* **1988**, *95*, 5558.

(27) Manolopoulos, D. E.; Stark, K.; Werner, H.-J.; Arnold, D. W.; Bradforth, S. E.; Neumark, D. M. *Science* **1993**, *262*, 1852.

(28) Morgner, H.; Seiberle, H. *Can. J. Chem.* **1994**, *72*, 995.

(29) Most of the Caltech publications to be referenced here (1976−1994) are collected in the following two volumes; Zewail, A. H. *Femtochemistry—Ultrafast Dynamics of the Chemical Bond*; World Scientific: Teaneck, NJ; Singapore; 1994. These references will not be detailed here because of the limited space available.

(30) Lambert, W. R.; Felker, P. M. *J. Chem. Phys.* **1981**, *75*, 5958. Felker, P. M.; Zewail, A. H. *Ibid.* **1985**, *82*, 2961, 2975, 2994, 3603.

(31) Baskin, J. S.; Felker, P. M.; Zewail, A. H. *J. Chem. Phys.* **1986**, *84*, 4708. Felker, P. M.; Zewail, A. H. Molecular Structures from Ultrafast Coherence Spectroscopy. In *Femtosecond Chemistry*; Manz, J., Wöste, L., Eds.; VCH: Weinheim, 1995 and references therein.

(32) Khundkar, L. R.; Knee, J. L.; Zewail, A. H. *J. Chem. Phys.* **1987**, *87*, 77. See also pp 97 and 115.

(33) Scherer, N. F.; Knee, J. L.; Smith, D. D.; Zewail, A. H. *J. Phys. Chem.* **1985**, *89*, 5141.

(34) Dantus, M.; Rosker, M. J.; Zewail, A. H. *J. Chem. Phys.* **1987**, *87*, 2395; **1988**, *89*, 6128.

(35) Zewail, A. H. *J. Phys. Chem.* **1993**, *97*, 12427.

(36) Zewail, A. H. In *Femtosecond Chemistry*; Manz, J., Wöste, L., Eds.; VCH: Weinheim, 1995, p 15.

experiments, the coherent wave packet contains information about all the molecular states involved. Accordingly, even for nonreactive systems, the observed motion of the packet can be transformed into an eigenstate spectrum with the vibrational and rotational states displayed: no loss of state resolution!

For reactions, the evolving wave packet moves into different regions of configurational space and may transform to another configuration or get trapped on its way to products. Observation of such dynamics in the transition state region requires isolation of the different elementary steps in time. Because the initial trajectories are all synchronized at zero time, a train of femtosecond pulses can probe them as they visit different regions, corresponding to different separations between atoms. Such probing is also a coherent process and has been achieved using a variety of detection methods on the femtosecond time scale, including absorption, laser-induced fluorescence, multiphoton-ionization mass spectrometry, photoelectron spectroscopy, and stimulated-emission pumping.[29,37-40] More recently, ultrafast electron diffraction has been introduced as a method for complementing the spectroscopic probing approach, especially for complex reactive systems.[29]

Historically, the concept of coherent wave packet motion in molecular systems has its roots in the experimental observation of quantum coherence among the vibrational states of large *isolated* molecules.[30] In 1980, picosecond preparation of vibrational coherence in a beam of isolated anthracene (72 normal modes) illustrated this concept; quantum coherence was observed as the system evolved in time from the initial to the final state with well-defined period and phase. With shorter time resolution, such an idea, applied to chemical reaction dynamics (in 1985), became a key concept for probing the transition states and their structural changes with femtosecond resolution. The state of the art in time resolution is currently ~6 fs.

Applications to different classes of reactions in different phases are numerous in many laboratories around the world; here, we limit ourselves to some examples from the Caltech group.[29,35,36] The specific examples given are chosen to span classes of reactions which display different structures and dynamics in the transition state region.

1. Dissociation Reactions. One example that illustrates the methodology and the concept of femtosecond transition state spectroscopy is the dissociation reactions of alkali halides (see section II).[29] For these systems, the covalent (M + X, where M denotes the alkali atom and X the halogen) potential and the ionic ($M^+ + X^-$) potential cross at an internuclear separation larger than 3 Å. The reaction coordinate therefore changes character from being covalent at short distances to being ionic at larger distances. The reaction occurs by a harpoon mechanism and has a large cross section because of the involvement of the ionic potential.

In studying this system, the first femtosecond pulse takes the ion pair M^+X^- to the covalent "bonded" MX potential at a separation of 2.7 Å. The activated complexes $[MX]^{*‡}$, following their coherent preparation, increase their internuclear separation and ultimately transform into the ionic $[M^+\cdots X^-]^‡$ form. With a series of pulses, delayed in time from the first one, the nuclear motion through the transition state and all the way to the final M + X products can be followed. The probe pulse examines the system at an absorption frequency corresponding to either the complex $[M\cdots X]^{*‡}$ or the free atom M.

Figure 5 gives the observed transients of the NaI reaction for the two detection limits. The resonance along the reaction coordinate reflects the motion of the wave packet when the activated complexes are monitored at a certain internuclear separation. The steps describe the quantized buildup of free Na, with separations matching the resonance period of the activated complexes. The complexes do not dissociate on every outbound pass, since there is a finite probability that the I atom can be harpooned again when the Na···I internuclear separation reaches the crossing point at 7 Å. The complexes survive for about 10 oscillations before completely dissociating to products. When the position of the crossing point is adjusted by changing the difference in the ionization potential of M and the electronegativity of X, e.g., NaBr, the survival of the complex changes (NaBr complexes, e.g., survive for only 1 period).

The results in Figure 5 illustrate additionally some important features of the dynamics. The oscillatory motion is damped, in a quantized fashion, and this damping is due to the *bifurcation* of the wave packet at the crossing point of the covalent and ionic potentials, as shown in the quantum calculation given in the figure. In fact, it is this damping which provides important parts of the dissociation dynamics, namely, the reaction time, the probability of dissociation, and the extent of covalent and ionic characters in the bond. These observations and their analyses have been made in more detail elsewhere,[29,35,36] and other systems have been examined similarly. Numerous theoretical studies of these systems have been made to test quantum, semiclassical, and classical descriptions of the reaction dynamics and to compare theory with experiment.

2. Isomerization Reactions. For systems with a large number of degrees of freedom (N), the situation is more complex. First, perpendicular to the reaction coordinate, there are now $N - 1$ possible motions. Second, the wave packet may suffer fast spreading as its structure is made of a large number of modes. The isomerization of diphenylethylene (stilbene) is an example of such a reaction with 72 modes: The reaction coordinate is usually described by a single motion about the double bond (torsional angle θ). The molecule at the *cis* configuration is essentially unbound in the θ coordinate but, in principle, is bound along all the other coordinates; a saddle-point transition state is defined.

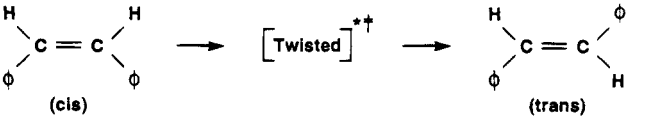

The wave packet was initially prepared by a femtosecond pulse (Figure 6). The temporal evolution was then probed by resonance multiphoton ionization.[29] The transient exhibits an exponential decay (reaction

(37) Baumert, T.; Gerber, G. *Isr. J. Chem.* **1994**, *34*, 103 and references therein. Also: Gerber et al. in ref 36, p 397.
(38) Glownia, J.; Misewich, J.; Walkup, R.; Kaschke, M.; Sorokin, P. *Top. Appl. Phys.* **1992**, *70*, 1 and references therein.
(39) Chen, Y.; Hunziker, L.; Ludowise, P.; Morgen, M. *J. Chem. Phys.* **1992**, *97*, 2149.
(40) For a collection of recent examples, see: *Ultrafast Phenomena VIII*; Martin, J. L., Migur, A., Mourou, G. A., Zewail, A. H., Eds.; Springer-Verlag: New York, 1993.

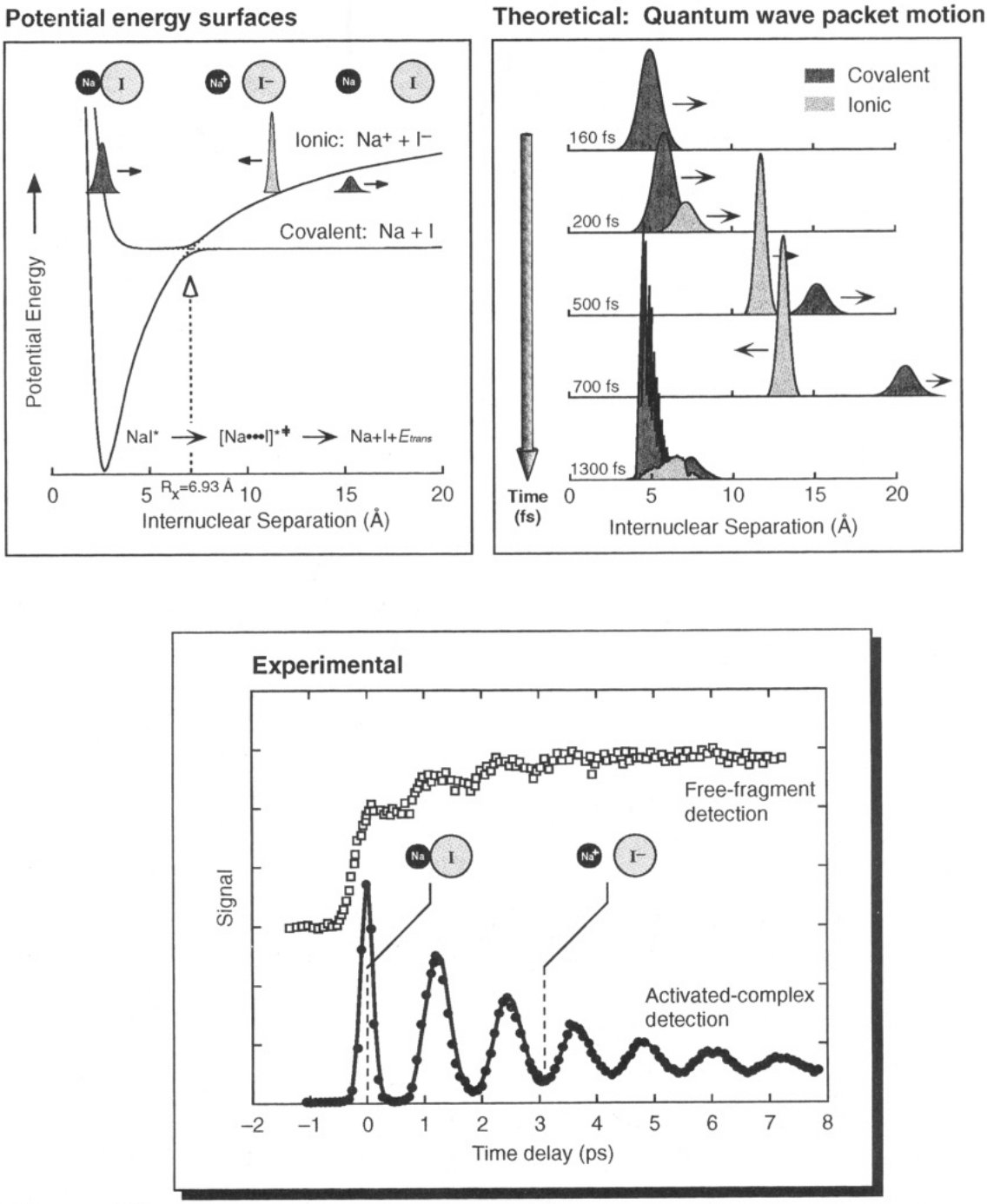

Figure 5. Femtosecond dynamics of dissociation (NaI) reaction. Bottom: Experimental observations of wave packet motion, made by detection of the activated complexes [NaI]*‡ or the free Na atoms. Top: Potential energy curves (left) and the "exact" quantum calculations (right) showing the wave packet as it changes in time and space. The corresponding changes in bond character are also noted: covalent (at 160 fs), covalent/ionic (at 500 fs), ionic (at 700 fs), and back to covalent (at 1.3 ps). Adapted from the following: Rose, T. S.; Rosker, M. J.; Zewail, A. H. *J. Chem. Phys.* **1988**, *88*, 6672; **1989**, *91*, 7415. Engel, V.; Metiu, H.; Almeida, R.; Marcus, R. A.; Zewail, A. H. *Chem. Phys. Lett.* **1988**, *152*, 1.

time) and an oscillatory pattern. The PES and trajectory in Figure 6 illustrate the molecular changes and corresponding structures. In the twisting of the double bond there are at least three angular coordinates, out of the 72 modes, directly involved: the C_e-C_e torsional angle, θ reaction coordinate; the $C_e-C_e-C_{Ph}$ in-plane bending angle, α; and the C_e-C_{Ph} torsional angle, ϕ.

To compare with experiments, molecular dynamics calculations were made by solving the equation of motion, starting from $t = 0$ and on until complete isomerization. Two time scales are involved: one for the initial dephasing of the packet (tens of femtoseconds) and the other for the relatively slower (hundreds of femtoseconds) nuclear dynamics of twisting. The reaction coordinate involves the θ as well as α and ϕ coordinates, as shown for the reaction trajectory and structures displayed in Figure 6. The total reaction time toward twisting is ~300 fs.

This type of coherent twisting motion is now evident in other systems,[40,41] and remarkably this same resonance behavior of the motion in N-dimensional space was also observed for stilbene in solution.[41] The

(41) Raftery, D.; Sension, R. J.; Hochstrasser, R. M. In *Activated Barrier Crossing*; Fleming, G. R., Hänggi, P., Eds.; World Scientific: Teanect, NJ, Singapore, 1993; p 163. Sundström, V. Work to be published.

(42) Wang, Q.; Schoenlein, R. W.; Peteanu, L. A.; Mathies, R. A.; Shank, C. V. *Science* **1994**, *266*, 422 and references therein.

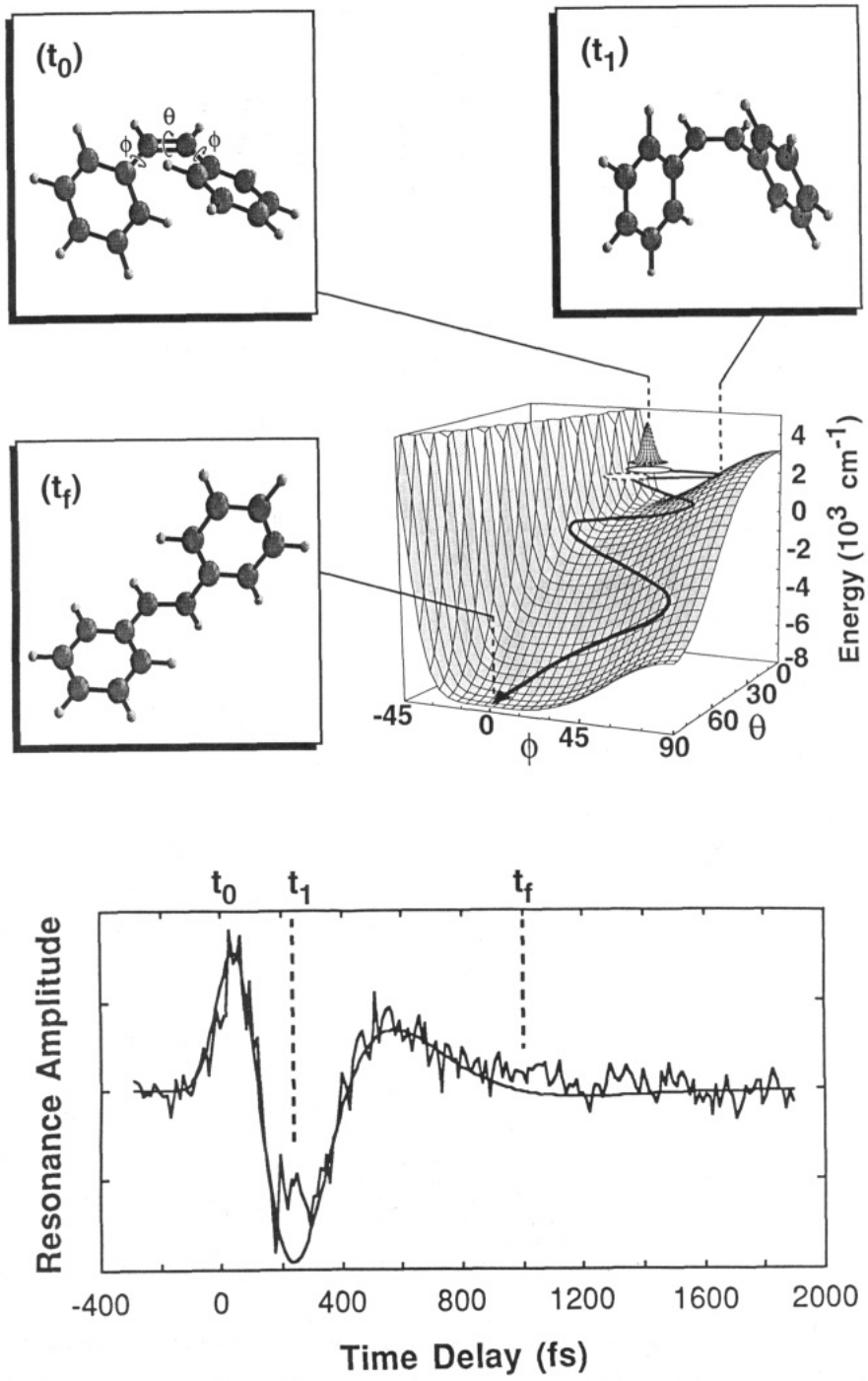

Figure 6. Femtosecond dynamics of isomerization (stilbene) reaction. Bottom: Experimental observation of the twisting (decay) and resonance (oscillation) motions depicted on the PES (middle). The trajectory shown on the PES describes the changes in the molecular structure, and three snapshots at different times display the corresponding structures. Adapted from the following: Pedersen, S.; Bañares, L.; Zewail, A. H. *J. Chem. Phys.* **1992**, *97*, 8801.

phenomenon is also evident in more complex biological systems, e.g., isomerization of rhodopsin,[42] the key primary event of vision.

3. Barrier Reactions. The simplest system for addressing the dynamics of barrier reactions is of the type $[ABA]^{\ddagger} \rightarrow AB + A$. This system is the half-collision of the A + BA full collision (see Figure 8). It involves one symmetrical stretch (Q_s), one asymmetrical stretch (Q_a), and one bend (q); it defines a barrier along the reaction coordinate.

The "lifetime" of the transition state over a saddle point near the top of the barrier is the most probable time for the system to stay near this configuration. It is simply expressed, for a one-dimensional reaction coordinate (frequency ω) near the top of the barrier, as $\tau^{\ddagger} = 1/\omega$. For values of $\hbar\omega$ from 50 to 500 cm^{-1}, $\tau^{\ddagger}$ ranges from 100 to 10 fs. In addition to this motion, one must include the transverse motion perpendicular to the reaction coordinate, with possible vibrational resonances, as discussed in section III.2.

The IHgI system, representing this class of reactions, has been studied with femtosecond resolution.[29] The activated complexes $[IHgI]^{*\ddagger}$, for which the asymmetric (translational) motion gives rise to vibrationally cold (or hot) nascent HgI, were prepared coherently at the crest of the energy barrier (Figure 7). The barrier-descent motion was then observed using series of probe pulses.

As the bond of the activated complexes breaks during the descent, both the *vibrational motion (~300*

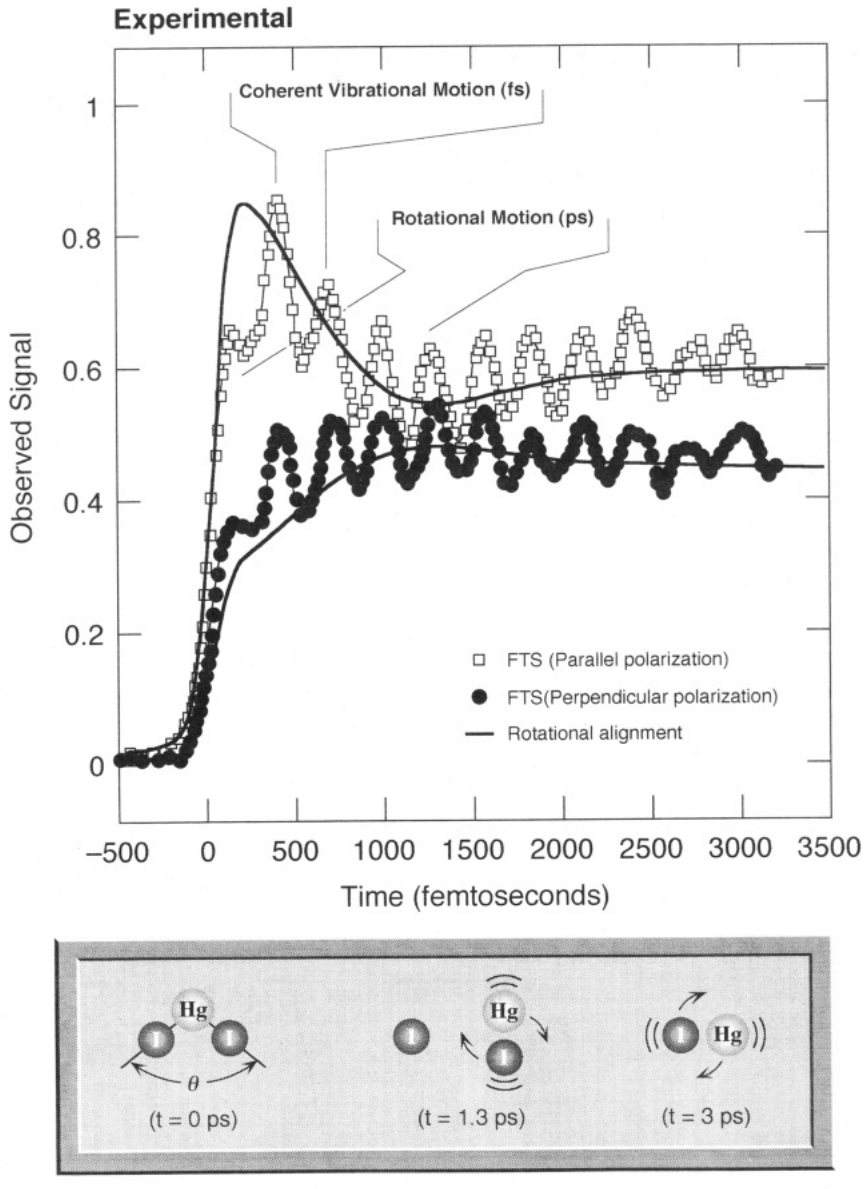

Figure 7. Femtosecond dynamics of barrier reactions. (a, left) Experimental observation of the vibrational (femtosecond) and rotational (picosecond) motions for the barrier (saddle-point transition state) descent, $[IHgI]^{*\ddagger} \rightarrow HgI(vib, rot) + I$. The vibrational coherence in the reaction trajectories (oscillations) is observed in both polarizations of FTS (femtosecond transition state spectra). The rotational orientation can be seen in the decay of FTS (parallel) and buildup of FTS (perpendicular) as the HgI rotates during bond breakage (bottom). (b, right) Potential energy surfaces, with a trajectory showing the coherent vibrational motion as the diatom separates from the I atom. Two snapshots of the wave packet motion (quantum molecular dynamics calculations) are shown for the same reaction at $t = 0$ and $t = 600$ fs. Adapted from the following: Dantus, M.; Bowman, R. M.; Gruebele, M.; Zewail, A. H. *J. Chem. Phys.* **1989**, *91*, 7437. Gruebele, M.; Roberts, G.; Zewail, A. H. *Philos. Trans. R. Soc. London, A* **1990**, *332*, 223.

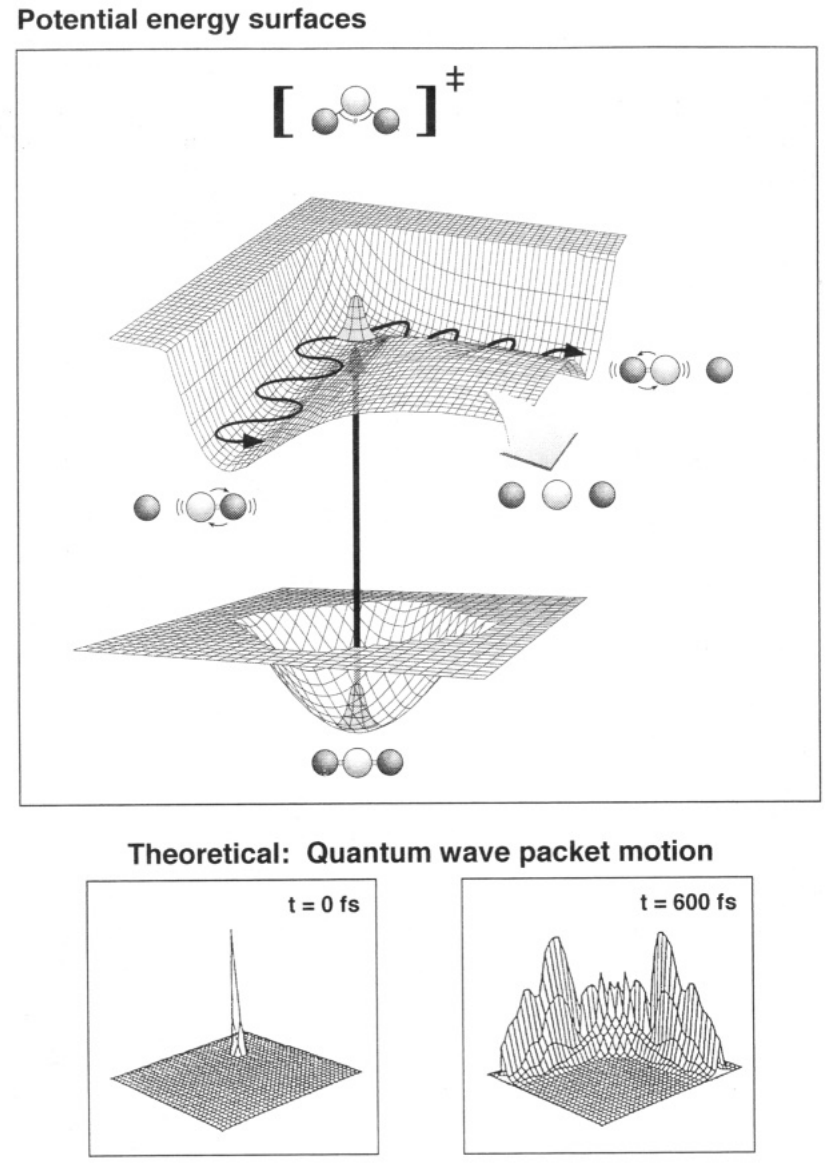

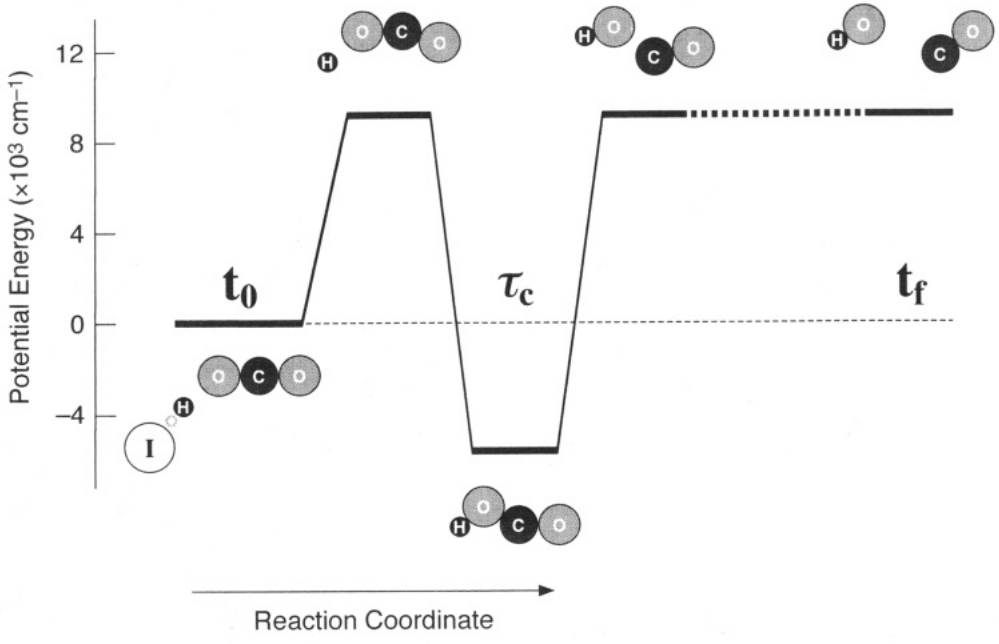

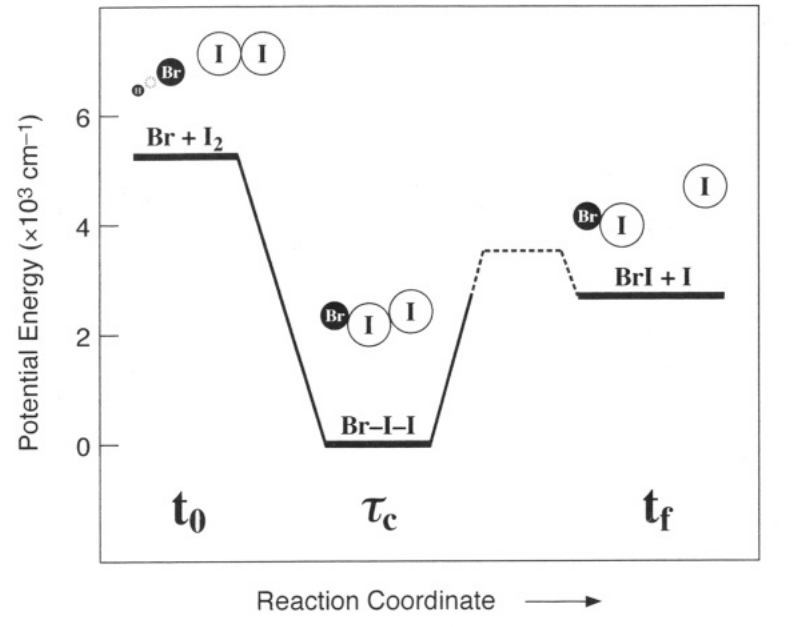

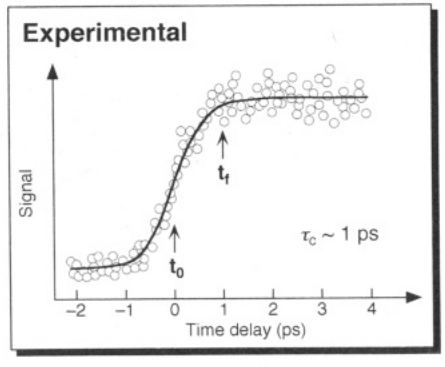

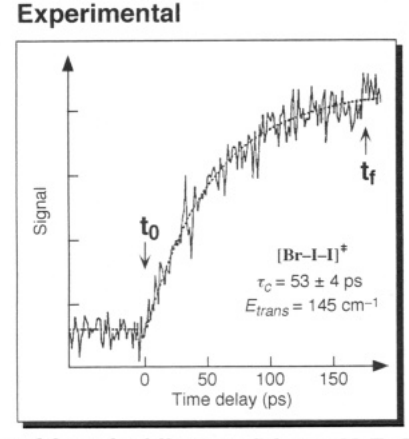

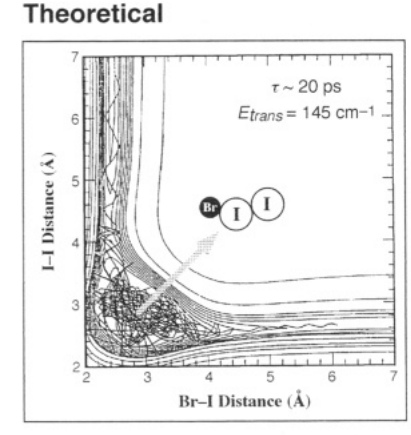

Figure 8. Femtosecond dynamics of abstraction (H + CO_2 → OH + CO) and exchange (Br + I_2 → BrI + I) reactions. (a, left) The PES along the reaction coordinate, and the observed rise of the OH from the breakup of the collision complex [HOCO]‡; lifetime $\tau_c \sim 1$ ps. The corresponding structures are noted with emphasis on three snapshots t_0, τ_c, and t_f (final) at the asymptote region. (b, right) Similar to part a but for the exchange reaction. Here, τ_c = 53 ps, and as shown in theoretical molecular dynamics the [BrII]‡ complex is trapped in a well. Adapted from the following: Scherer, N. F.; Khundkar, L. R.; Bernstein, R. B.; Zewail, A. H. *J. Chem. Phys.* **1987**, *87*, 1451. Scherer, N. F.; Sipes, C.; Bernstein, R. B.; Zewail, A. H. *Ibid.* **1990**, *92*, 5239. Ionov, S. I.; Brucker, G. A.; Jaques, C.; Valachovic, L.; Wittig, C. *Ibid.* **1993**, *99*, 6553. Sims, I. R.; Gruebele, M.; Potter, E. D.; Zewail, A. H. *Ibid.* **1992**, *97*, 4127. Wittig, C.; Zewail, A. H. In *Chemical Reactions in Clusters*; Bernstein, E., Ed.; Oxford University Press: Oxford, 1995.

fs), of the separating diatom, and the *rotational motion (~1.3 ps)*, caused by the torque, can be observed (Figure 7). These studies of the dynamics provided the initial geometry of the transition state, which was found to be bent, and the nature of the final torque which induces rotations in the nascent HgI fragment. Classical and quantum molecular dynamics simulations[29] show the important features of the dynamics and the nature of the force acting during bond breakage. Two snapshots are shown in Figure 7.

The force controls the remarkably persistent (observed) *coherence in products*, a feature which was unexpected, especially in view of the fact that all trajectory calculations are normally averaged (by Monte Carlo methods) without such coherences. Only recently has theory addressed this point.[43-45] The same type of coherence along the reaction coordinate, first observed[29] in 1987, was found for reactions in solutions,[40,46,47] in clusters,[37,48-50] and in solids,[51] offering a new opportunity for examining solvent effects on reaction dynamics in the transition state region.

Even more surprising was the fact that this same phenomenon was also found to be common in biological systems, where the *products* were formed coherently in the twisting of a bond, e.g., in bacteriorhodopsin;[42] the breakage of a bond, e.g., in ligand–myoglobin[52] systems; and in electron and excitation transfer, e.g., in photosynthetic reaction centers[53] and the light-harvesting pigment–protein[54] complexes. The implications as to the global motion of the protein are fundamental to the understanding of the mechanism (coherent *vs.* statistical energy or electron flow), and such new observations are triggering new theoretical studies in these biological systems.[55]

4. Abstraction and Exchange Reactions. Real-time clocking of abstraction reactions was first performed on the I–H/CO_2 system for the dynamics on the *ground-state* PES:[29]

$$H + CO_2 \rightarrow [HOCO]^{\ddagger} \rightarrow CO + OH$$

Two pulses were used, the first to initiate the reaction and the second delayed to probe the OH product. The decay of $[HOCO]^{\ddagger}$ was observed in the buildup of the OH final fragment in real time. The two reagents were synthesized in a van der Waals complex, following the methodology discussed in section II. The PES along the reaction coordinate and results (at one energy) are shown in Figure 8. The results showed that the reaction involves a *collision complex* and that the lifetime of $[HOCO]^{\ddagger}$ is relatively long, about a picosecond.

Wittig's group[56] has recently made a significant step forward and reported accurate rates with sub-picosecond resolution, covering a sufficiently large energy range to test the description of the lifetime of $[HOCO]^{\ddagger}$ by an RRKM theory. Recent crossed molecular beam studies of OH and CO, from the group in Perugia (Italy),[57] have shown that the angular distribution is consistent with a long-lived complex. Vector-correlation studies by the Heidelberg group[58] addressed the importance of the lifetime to IVR and to product state distributions. The molecular dynamics calculations (on *ab initio* potentials) by Clary and Schatz[59] are also consistent with such lifetimes of the complex and provide new insight into the effect of energy, rotations, and resonances on the dynamics of $[HOCO]^{\ddagger}$. This is one of the reactions in which both theory and experiment have been examined in a very critical and detailed manner.

For exchange reactions, the femtosecond dynamics of bond breaking and bond making was examined in the following system:[29]

$$Br + I_2 \rightarrow [BrII]^{\ddagger} \rightarrow BrI + I$$

The dynamics of this Br + I_2 reaction (Figure 8) was resolved in time by detecting the BrI with the probe pulses using laser-induced fluorescence. The reaction was found to be going through a sticky (tens of picoseconds) collision complex. More recently, McDonald's group[60] has monitored this same reaction, using multiphoton-ionization mass spectrometry, and found the rise of I (and I_2) to be, within experimental error, similar to the rise of BrI (Figure 8). With molecular dynamics simulations, comparison with the experimental results showed the trapping of trajectories in the $[BrII]^{\ddagger}$ potential well; the complex is a stable molecular species in a picosecond bottle!

Gruebele et al. (see ref 29) drew a simple analogy between collision (Br + I_2) and half-collision ($h\nu$ + I_2) dynamics based on the change in bonding and using frontier orbitals to describe it.[61] *Ab initio* and dynamics calculations are now rigorous enough to allow for direct comparison of theory and experiment.

5. Addition, Cleavage, and Elimination Reactions. For more than a century,[62] one of the most well-studied addition/elimination reactions, both theoretically and experimentally, is the ring opening of cyclobutane to yield ethylene or the reverse addition of two ethylenes to form cyclobutane (Figure 9). Such is a classic case study for a Woodward–Hoffmann description of *concerted* reactions. The reaction, however, may proceed directly through a transition state at the saddle region of an activation barrier, or it could proceed with a diradical intermediate, beginning with

(43) Manz, J.; Reischl, B.; Schroeder, T.; Seyl, F.; Wartmuth, B. *Chem. Phys. Lett.* **1992**, *198*, 483. Burghardt, I.; Gaspard, P. *J. Chem. Phys.* **1994**, *100*, 6395.
(44) Ben-Nun, M.; Levine, R. D. *Chem. Phys. Lett.* **1993**, *203*, 450.
(45) Metiu, H. *Faraday Discuss. Chem. Soc.* **1991**, *91*, 249 and earlier references therein.
(46) See: Ruhman, S.; Fleming, G.; Hochstrasser, R.; Nelson, K.; Mathies, R.; Shank, C.; Barbara, P.; Wiersma, D. In *Femtosecond Reaction Dynamics*; Wiersma, D. A., Ed.; Royal Netherlands Academy of Arts & Sciences; North-Holland: Amsterdam, 1994.
(47) Banin, U.; Bartana, A.; Ruhman, S.; Kosloff, R. *J. Chem. Phys.* **1994**, *101*, 8461 and references therein.
(48) Papanikolas, J. M.; Vorsa, V.; Nadal, M. E.; Campagnola, P. J.; Gord, J. R.; Lineberger, W. C. *J. Chem. Phys.* **1992**, *97*, 7002.
(49) Liu, Q.; Wang, J.-K.; Zewail, A. H. *Nature (London)* **1993**, *364*, 427. Potter, E. P.; Liu, Q.; Zewail, A. H. *Chem. Phys. Lett.* **1992**, *200*, 605.
(50) Kühling, H.; Kobe, K.; Rutz, S.; Schreiber, E.; Wöste, L. *J. Phys. Chem.* **1994**, *98*, 6679.
(51) Zadoyan, R.; Li, Z.; Ashjian, P.; Martens, C. C.; Apkarian, V. A. *Chem. Phys. Lett.* **1994**, *218*, 504.
(52) Zhu, L.; Sage, J. T.; Champion, P. M. *Science* **1994**, *266*, 629.
(53) Martin, J. L.; Breton, J.; Vos, M. H. in ref 46. See also: Vos, M. H.; et al. *Nature (London)* **1993**, *363*, 320.
(54) Chachisvilis, M.; Pullerits, T.; Jones, M. R.; Hunter, C. N.; Sundström, V. *Chem. Phys. Lett.* **1994**, *224*, 345.
(55) Gehlen, J. N.; Marchi, M.; Chandler, D. *Science* **1994**, *263*, 499 and other references therein.
(56) Ionov, S. I.; Brucker, G. A.; Jaques, C.; Valachovic, L.; Wittig, C. *J. Chem. Phys.* **1993**, *99*, 6553.
(57) Alagia, M.; Balucani, N.; Casavecchia, P.; Stranges, D.; Volpi, G. G. *J. Chem. Phys.* **1993**, *98*, 8341.
(58) Jacobs, A.; Volpp, H.-R.; Wolfrum, J. *Chem. Phys. Lett.* **1994**, *218*, 51.
(59) Clary, D. C.; Schatz, G. C. *J. Chem. Phys.* **1993**, *99*, 4578. Hernández, M. I.; Clary, D. C. *J. Chem. Phys.* **1994**, *101*, 2779.
(60) Wright, S. A.; Tuchler, M. F.; McDonald, J. D. *Chem. Phys. Lett.* **1994**, *226*, 570.
(61) Herschbach, D. R. *Angew. Chem., Int. Ed. Engl.* **1987**, *26*, 1221.
(62) Berson, J. *Science* **1994**, *266*, 1338 and references therein.

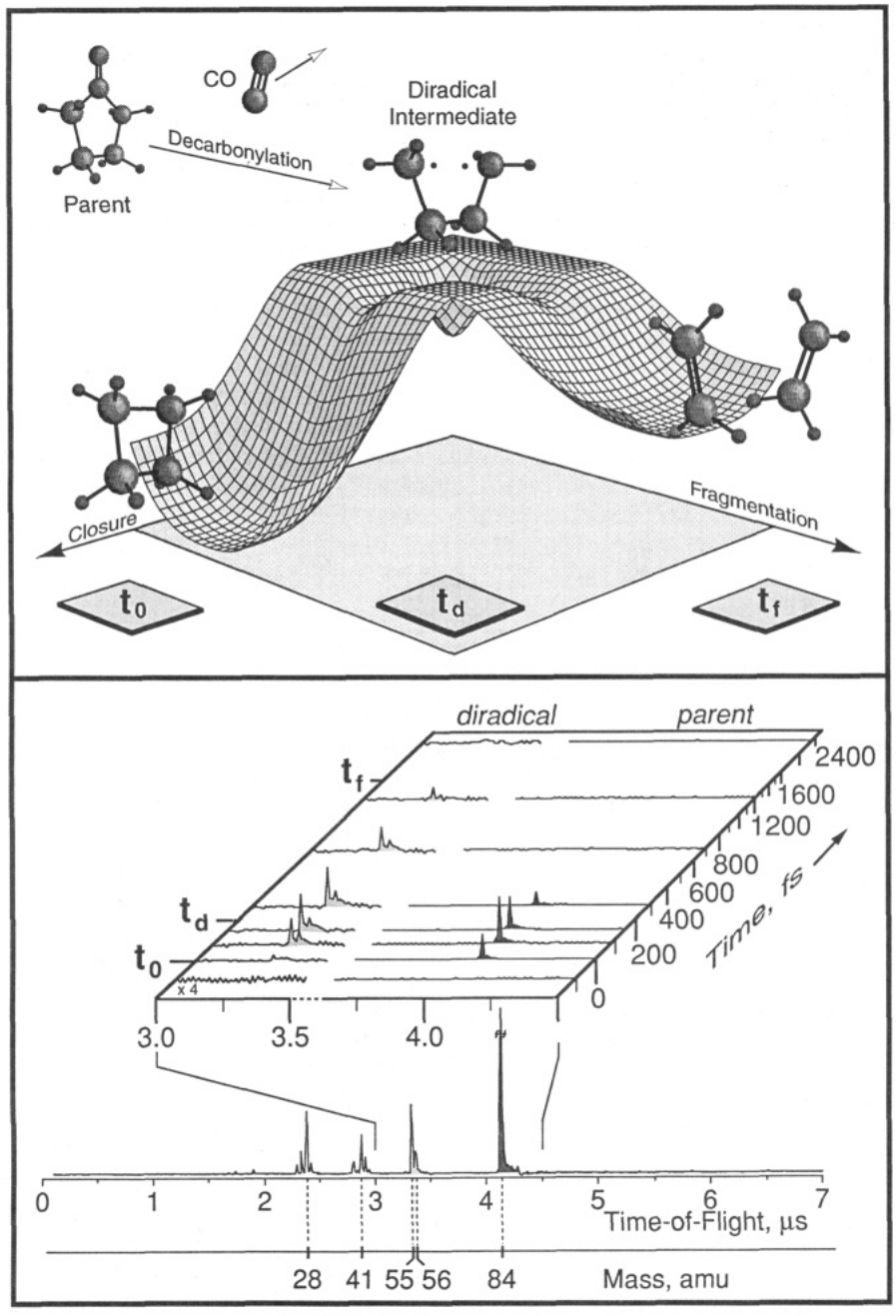

Figure 9. Femtosecond dynamics of addition/cleavage reaction of the cyclobutane–ethylene system. Bottom: Experimental observation of the intermediate diradical by mass spectrometry. Top: The PES showing the nonconcerted nature of the reaction, together with three snapshots of the structures at t_0 (initial), t_d (diradical), and t_f (final). The parent precursor is also shown. Adapted from the following: Pedersen, S.; Herek, J. L.; Zewail, A. H. *Science* **1994**, *266*, 1293.

the breakage of one σ-bond to produce tetramethylene, which in turn passes through a transition state before yielding final products. The concept, therefore, besides being important to the definition of diradicals as stable species, is crucial to the fundamental nature of the reaction dynamics: *a concerted one-step process vs a two-step process with an intermediate.*

Experimental and theoretical studies have long focused on the possible existence of diradicals and on the role they play in affecting the processes of cleavage, closure, and rotation. The experimental approach is based primarily on studies of the stereochemistry of reactants and products, chemical kinetics, and the effect of different precursors on the generation of diradicals. The time "clock" for rates is internal, inferred from the rotation of a single bond, and is used to account for any retention of stereochemistry from reactants to products. Theoretical approaches basically fall into two categories: those involving thermodynamical analysis of the energetics (enthalpic criterion) and those concerned with semiempirical or *ab initio* quantum calculations of the PES describing the motion of the nuclei.

It appears, therefore, that real-time studies of these reactions should allow one to examine the nature of the transformation and the validity of the diradical hypothesis. In recent work, the Caltech group[63] reported direct studies of the femtosecond dynamics of the transient diradical structures. The aim was at "freezing" the diradicals in time, in the course of the reaction. Various precursors were used to generate the diradicals and to monitor the formation and the decay dynamics of the reaction intermediate(s). The parent (cyclopentanone) or the intermediate species

(63) Pedersen, S.; Herek, J. L.; Zewail, A. H. *Science* **1994**, *266*, 1359.

was distinctly identified using time-of-flight mass spectrometry. The concept behind the experiment and some of the results are given in Figure 9.

The mass spectrum obtained at different femtosecond time delays shows the changes of the intermediates. At negative times there is no signal present. At time zero, the parent mass (84 amu) of the precursor cyclopentanone is observed, while the intermediate mass of 56 amu is not apparent. As the time delay increases, a *decrease* of the 84 mass signal was observed and, for the 56 mass, first the *increase* and then the *decrease* of the signal. The 56 mass corresponds to the parent minus the mass of CO, and its dynamics directy reflects the nature of the transition state region.

Considering the dynamics of nuclei at the top of the barrier, it is impossible at these velocities to obtain such time scales if a wave packet is moving translationally on a "flat" surface. For example, over a distance of 0.5 Å, which is significantly large on a bond scale, the time in the transition state region will be ~40 fs. The reported (sub)picosecond times therefore reflect the involvement of other nuclear degrees of freedom. In the original publication[63] the rates were related to the stability of the diradical species. By varying the total energy and using different substituents, these studies gave a direct evidence that the diradical is a stable species on the global PES. The discovery of their time scales and elementary dynamics defines the mechanistic concept, crucial to the understanding of the nature of the chemical change, the stereochemistry, and product selectivity. The approach is general for the study of other reactive intermediates in reactions.

Using the same techniques, elimination reactions were clocked[29] in order to address a similar problem: the nature of two-center elimination by either a *one-step* or a *two-step* process. The reaction of interest is

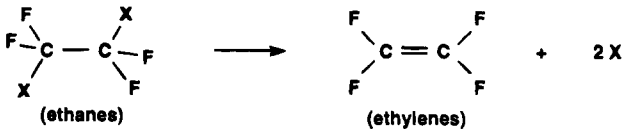

where the 2X (in this case 2I) elimination leads to the transformation of ethanes to ethylenes. The questions then are: Do these similar bonds break simultaneously or consecutively with formation of intermediates? What are the time scales?

Methyl iodide's C–I nonbonding to antibonding orbital transition (at ~2800 Å) is known to fragment and form iodine in both spin–orbit states (I and I*). The CH_3 fragment produced is vibrationally excited. In both I and I* channels, the iodine atoms rise in a time of less than 0.5 ps. For $I-CF_2-CF_2-I$, the situation is entirely different. The bond breakage, which leads to elimination, is consecutive, nonconcerted: primary bond breakage (~200 fs) similar to that of methyl iodide and a much slower (32 ps) secondary bond breakage. The dynamics of the prompt breakage can be understood by applying the theoretical techniques mentioned above for coherent wave packet motion in direct dissociation reactions,[29] but what determines the dynamics of the slower secondary process?

The observation of a 30 ps rise, by monitoring I, indicates that, after the recoil of the fragments in the primary fragmentation, the total internal energy in the intermediate $[CF_2I-CF_2]^{\ddagger}$ is sufficient for it to undergo secondary dissociation and produce I in the ground state. From the photon energy (102 kcal mol^{-1}) used in the experiment, the C–I bond energy (52.5 kcal mol^{-1}), and the mean translational energy of similar systems (obtained by Lee's group),[64] the internal energy of the fragment was found to be comparable with the activation energy. The $(30\ ps)^{-1}$ represents the average rate for this secondary bond-breaking process (barrier 3–5 kcal mol^{-1}).

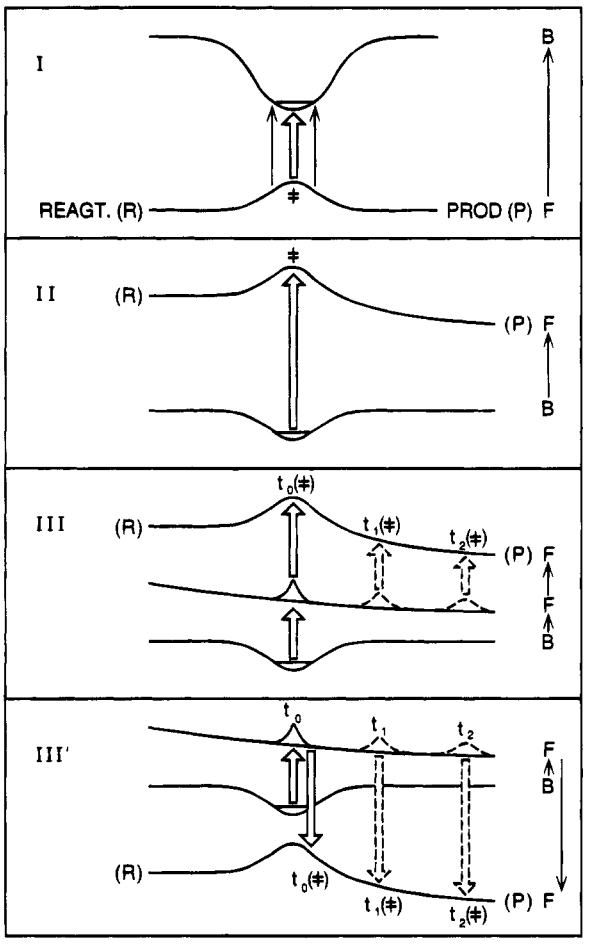

Figure 10. Schematic diagrams of potential energy curves in four schemes for transition state spectroscopy (see text); I and II have been implemented; III and III' are proposed here. The reactive PES is indicated in each case by the fact that it is a free state F that links reagents (R) to products (P). Vertical arrows indicate optical transitions.

When the total energy was changed in these experiments, the decay became slower than 30 ps as energy decreased. This energy dependence of the process could be understood considering the time scale for IVR and the microcanonical rates, $k(E)$ at a given energy, in a statistical RRKM description. This dynamics of consecutive bond breakage is common to many systems and also relevant to the mechanism in different classes of reactions discussed in the organic literature.

IV. Dreaming of the Transition State

This section offers a bridge between the present and the future. Thus in Figure 10 the first two schemes shown for TSS are ones that have been implemented. (In this figure upward arrows indicate laser absorption, and downward, laser-stimulated emission).

(64) Lee, Y. T. *Science* **1987**, *236*, 793.

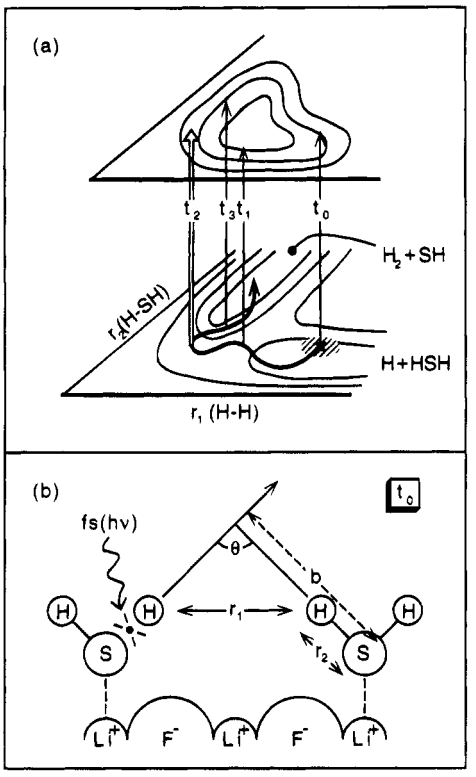

Figure 11. (a) Scheme I of Figure 10 in greater detail. If the trajectories across the lower (reactive free) state originate in a localized region (shaded), then the system will conform to a restricted path, as indicated. This can be interrogated at successive times t_0, t_1, ..., etc. by time-resolved excitation to the excited bound state. Lingering of the trajectory at a turning point is shown leading to enhanced absorption at t_2. (b) The necessary restriction of initial state geometry (r_1(H−H), r_2(H−SH), θ, and b) is shown schematically in the lower panel as being achieved by way of surface-aligned femtosecond photoreaction in H_2S(ad)/LiF(001) starting at time t_0.

Scheme I, in which excitation is from the free state of interest, F, to a bound state, B, has the drawback that there exists a broad range of pathways from reagents to products on state F, as well as a correspondingly broad TS spectrum. Scheme II corrects this by binding the particles as a neutral or charged complex on a lower PES, B, and then exciting to the state of interest, F. The drawback to this otherwise successful scheme is that only a limited range of TS configurations (‡) are accessed. The new postulated schemes III and III′ (based on the time-resolved procedures of section III above) suggest ways of rectifying this for reaction across an electronically excited PES (III) or a ground state PES (III′). In each case an intermediate repulsive state is used to scan through successive TS's (‡) and thereby map a broad region of the PES.

In Figure 11 we make the point that TSS starting in the reagent valley of the PES, as envisaged in the original scheme for TSS (Figure 10, scheme I), could be feasible and informative if the reagents were constrained as to initial separation, collision angle, and impact parameter and the spectrum was recorded at successive times. The method proposed for constraining the reagents (Figure 11b) is their coadsorption at low temperature on an inert crystal (LiF in the illustration).[24] In the example illustrated, illumination with UV triggers the reaction H + H_2S(ad) → H_2(g) + HS(ad),[65] with the zero time configuration now well-defined.

The dream goes beyond understanding of the PES, to control of the reaction pathway. Here the field can build on early successes. Energy transfer from electronic to vibrational degrees of freedom in a Na*(3^2P) + H_2(v) collision can be controlled by exciting the atomic sodium wing absorption during the course of a Na + H_2 collision in the ground electronic state. The vibrational distribution of the product, H_2(v), has been altered substantially by exciting at various points in the red wing of the Na.[66]

A series of studies of far-wing absorption in M + H_2 (M = metal) collisions have extended this approach to the control of reactive as opposed to energy-transfer pathways.[67,68] Excitation of various wavelengths in the blue wing of Na + H_2 (→Na(4^2P)) resulted in order-of-magnitude changes in the ratio of reaction (→NaH (v = 1; J = 3, 4, 11)) to quenching (→Na(3^2P) + H_2). This was thought to be due to the effect that changing TS configuration on the upper PES had on the extent of barrier crossing to yield NaH.

In real time, the clocking of the wave packet motion has been exploited to control the yield of a reaction product or reaction channel. Two examples have been reported; one involved the unimolecular dissociation of alkali halides (section III.1), and the second was the harpooning reaction of Xe + I_2.[69] In the unimolecular reaction case, a third, timed controlling pulse was tuned to take the activated complexes [NaI]*‡ to a different reactive potential (Na* + I), by absorption, or to the ground state by stimulated emission, thus altering the branching of the Na + I *vs* Na* + I channels. For the Xe + I_2 reaction, the product yield was switched *on* or *off* by using a controlling pulse timed to take the wave packet to the harpoon region, which, once reached, led to the formation of product XeI*. The yield of XeI could thus be controlled. These types of experiments can also be extended to develop the mapping of collision configurations outlined in the schemes of Figures 10 and 11.

We make no attempt here at a comprehensive survey of the means of controlling reactive and inelastic encounters.[70] Control can evidently be achieved (a) by selecting a starting configuration in the TS region, $r^‡$; (b) by selecting a starting time, $t^‡$, relative to some other event, and thereby a phase, $\Phi^‡$; or (c) by manipulating the PES using a strong electric field to obtain $V^‡(\epsilon)$. An understanding of the geography of the wondrous landscape of the PES, obtainable through transition state spectroscopy, is clearly fundamental to every such undertaking.

This research was supported by the Natural Sciences and Engineering Research Council (NSERC) of Canada (to J.C.P.) and by the U.S. National Science Foundation and Air Force Office of Scientific Research (to A.H.Z.). We are grateful to Robert C. Jackson (Toronto) and Juen Kai Wang and Soren Pedersen (Pasadena) for help with the figures.

AR940090A

(65) Harrison, I.; Polanyi, J. C.; Young, P. A. *J. Chem. Phys.* **1988**, *89*, 1498.
(66) Hering, P.; Cunha, S. L.; Kompa, K. L. *J. Phys. Chem.* **1987**, *91*, 5459.
(67) Kleiber, P. D.; Lyyra, A. M.; Sando, K. M.; Zafiropulos, V.; Stwalley, W. C. *J. Chem. Phys.* **1986**, *85*, 5493.
(68) Bililign, S.; Kleiber, P. D.; Kearney, W. R.; Sando, K. M. *J. Chem. Phys.* **1991**, *96*, 218. Kleiber, P. D.; Stwalley, W. C.; Sando, K. M. *Annu. Rev. Phys. Chem.* **1993**, *44*, 13.
(69) Potter, E. D.; Herek, J. L.; Pedersen, S.; Liu, Q.; Zewail, A. H. *Nature (London)* **1992**, *355*, 66. Herek, J. L.; Materny, A.; Zewail, A. H. *Chem. Phys. Lett.* **1994**, *228*, 15. Zewail, A. H. *Phys. Today* **1980**, *33*, 27.
(70) See also the article on "control" by Kent R. Wilson and co-workers in this issue: Kohler, B.; Krause, J. L.; Raksi, F.; Wilson, K. R.; Yakovlev, V. V.; Whitnell, R. M.; Yan, Y. *Acc. Chem. Res.* **1995**, *28*, 133−140.